

# Exact Computation of LTI Reach Set from Integrator Reach Set with Bounded Input

Shadi Haddad, Pansie Khodary, Abhishek Halder

**Abstract**—We present a semi-analytical method for exact computation of the boundary of the reach set of a single-input controllable linear time invariant (LTI) system with given bounds on its input range. In doing so, we deduce a parametric formula for the boundary of the reach set of an integrator linear system with time-varying bounded input. This formula generalizes recent results on the geometry of an integrator reach set with time-invariant bounded input. We show that the same ideas allow for computing the volume of the LTI reach set.

## I. INTRODUCTION

Motivated by safety and performance verification of controlled dynamical systems, a vast body of works in systems-control literature have studied the problem of computing or approximating the reach sets in general, and the reach sets for linear control systems [1]–[7] in particular. See [8] for a recent survey on this broad topic.

For our purpose, a working definition for “reach set” would be “the set of states that a controlled dynamical system can reach at a fixed time with given bounds on its input range”. We will make this precise in Sec. II-A.

In this study, we propose a new semi-analytical method to compute the reach set of a controllable single input LTI system with known bounds on its input range.

*Specific Contributions:*

- We show (Sec. II) how certain generalizations of recent results [9]–[11] on the exact geometry (e.g., boundary, volume) of integrator reach sets can enable computing the controllable LTI reach sets with bounded input. Our results reveal that the controllable canonical form serves as a bridge to transfer such geometric results from the integrator to the original state coordinates.
- To realize the aforementioned transfer, we derive the exact integrator reach set (Sec. III) and its volume (Sec. IV) with time-varying input range that is determined by the original LTI system. These generalizations should be of independent interest, e.g., in certifying reach set intersections in feedback linearized coordinates [12].

*Notations and Preliminaries:* We will use the finite set notation  $\llbracket n \rrbracket := \{1, 2, \dots, n\}$ . The symbols  $\text{vol}_n$ ,  $\det$ ,  $|\cdot|$ ,  $\langle \cdot, \cdot \rangle$  denote the  $n$  dimensional Lebesgue volume, the determinant, the absolute value, and the standard Euclidean inner product, respectively.

Shadi Haddad is with the Department of Applied Mathematics, University of California, Santa Cruz, CA 95064, USA, [shhaddad@ucsc.edu](mailto:shhaddad@ucsc.edu).

Pansie Khodary and Abhishek Halder are with the Department of Aerospace Engineering, Iowa State University, Ames, IA 50011, USA, [pkhodary, ahalder}@iastate.edu](mailto:{pkhodary, ahalder}@iastate.edu).

Consider a *controllable* single input LTI system

$$\dot{z} = Az + bv, \quad A \in \mathbb{R}^{n \times n}, \quad b \in \mathbb{R}^n, \quad (1)$$

with state  $z \in \mathbb{R}^n$  and input  $v \in \mathbb{R}$ . Let  $q^\top$  denote the last row of the inverse of its controllability matrix, and define the nonsingular matrix

$$M := \begin{pmatrix} q^\top \\ q^\top A \\ \vdots \\ q^\top A^{n-1} \end{pmatrix}. \quad (2)$$

As is well-known [13, Sec. 6], the invertible linear map  $z \mapsto x := Mz$  transforms (1) into a *controllable canonical form*

$$\dot{x} = A_{\text{con}}x + b_{\text{con}}v, \quad (3)$$

where

$$A_{\text{con}} := MAM^{-1} = \begin{pmatrix} 0 & 1 & 0 & \dots & 0 \\ 0 & 0 & 1 & \dots & 0 \\ 0 & 0 & 0 & \dots & 0 \\ \vdots & \vdots & \vdots & \ddots & \vdots \\ 0 & 0 & 0 & \dots & 1 \\ -c_0 & -c_1 & -c_2 & \dots & -c_{n-1} \end{pmatrix},$$

$$b_{\text{con}} := Mb = (0 \ 0 \ \dots \ 0 \ 1)^\top. \quad (4)$$

In particular,  $A_{\text{con}}$  is a *companion matrix* (see e.g., [14, p. 195]) whose last row is in terms of the (real) coefficients of the monic characteristic polynomial of  $A$ , given by

$$p(\lambda) := \lambda^n + c_{n-1}\lambda^{n-1} + \dots + c_1\lambda + c_0. \quad (5)$$

Letting  $c := (c_0, c_1, \dots, c_{n-1})^\top$ , we can succinctly write  $A_{\text{con}}$  in (4) as

$$A_{\text{con}} = \begin{bmatrix} \mathbf{0}_{(n-1) \times 1} & \mathbf{I}_{n-1} \\ -c^\top & \end{bmatrix}. \quad (6)$$

## II. BRUNOVSKY NORMAL FORM AND LTI REACH SET

### A. Main Idea

Defining a new input

$$u := -\langle c, x \rangle + v \quad (7)$$

further transforms (3) into the *Brunovsky normal a.k.a. the  $n$ th order integrator form* with state  $x$  and input  $u$ , given by

$$\dot{x} = A_{\text{int}}x + b_{\text{con}}u, \quad (8)$$

where  $\mathbf{x} \in \mathbb{R}^n$  and  $u \in \mathbb{R}$ , and

$$\mathbf{A}_{\text{int}} := \begin{bmatrix} \mathbf{0}_{(n-1) \times 1} & \mathbf{I}_{n-1} \\ \mathbf{0}_{1 \times n} & \end{bmatrix}. \quad (9)$$

Given initial condition  $\mathbf{z}_0 := \mathbf{z}(t=0)$  for (1), the same for (8) is  $\mathbf{x}_0 = \mathbf{M}\mathbf{z}_0$ .

For continuous bounded  $u$ , i.e.,  $u(\cdot) \in C([0, t])$  and  $u_{\min} \leq u(\cdot) \leq u_{\max}$ , the *integrator reach set*  $\mathcal{X}_t(\{\mathbf{x}_0\}) \subset \mathbb{R}^n$  is the set of states that the controlled dynamics (8) can reach at a fixed time  $t$  starting from  $\mathbf{x}_0 \in \mathbb{R}^n$ , i.e.,

$$\mathcal{X}_t(\{\mathbf{x}_0\}) := \{\mathbf{x}(t) \in \mathbb{R}^n \mid (8), \quad \mathbf{u}(s) \in [u_{\min}, u_{\max}] \\ \forall s \in [0, t]\}. \quad (10)$$

Likewise, for continuous bounded  $v$ , i.e.,  $v(\cdot) \in C([0, t])$  and  $v_{\min} \leq v(\cdot) \leq v_{\max}$ , the *LTI reach set* is

$$\mathcal{Z}_t(\{\mathbf{z}_0\}) := \{\mathbf{z}(t) \in \mathbb{R}^n \mid (1), \quad \mathbf{v}(s) \in [v_{\min}, v_{\max}] \\ \forall s \in [0, t]\}. \quad (11)$$

Thanks to the Lyapunov convexity theorem [15]–[18], the reach sets (10) and (11) are guaranteed to be compact, convex [19, Prop. 6.1], [3], and in particular, *zonoids*<sup>1</sup> [9]–[11].

In this work, we consider the case that  $v_{\min}, v_{\max}$  are constants, i.e., the LTI input in (1) has time-invariant bounds.

We propose to use the input correspondence (7) for explicitly computing (11) in two steps:

**step 1:** explicitly compute the (boundary of the compact) integrator reach set  $\mathcal{X}_t(\{\mathbf{M}\mathbf{z}_0\})$  for to-be-determined input range  $[u_{\min}(s), u_{\max}(s)] \forall s \in [0, t]$ .

**step 2:** compute  $\mathcal{Z}_t(\{\mathbf{z}_0\}) = \mathbf{M}^{-1}\mathcal{X}_t(\{\mathbf{M}\mathbf{z}_0\})$ .

For **step 1**, notice from (7) that even when the original control input range is time invariant, i.e.,  $v_{\min}, v_{\max}$  are constants, still the transformed input  $u$  has a time-varying range  $[u_{\min}(s), u_{\max}(s)] \forall s \in [0, t]$ . This is because the input correspondence (7) occurs via time-varying  $\mathbf{x}$ . Thus, we cannot apply recent results [9]–[11] explicitly characterizing the integrator reach set boundary with *time-invariant* input range.

To circumvent this difficulty, we observe that  $\forall s \in [0, t]$ , the *linear* state dependence in (7) allows us to write

$$u_{\min}(s) = -\langle \mathbf{c}, e^{s\mathbf{A}_{\text{con}}} \mathbf{M}\mathbf{z}_0 \rangle + I_{\min}(s), \quad (12a)$$

$$u_{\max}(s) = -\langle \mathbf{c}, e^{s\mathbf{A}_{\text{con}}} \mathbf{M}\mathbf{z}_0 \rangle + I_{\max}(s), \quad (12b)$$

where

$$I_{\min}(s) := \inf_{v(\cdot) \in C([0, s])} I(v) \quad (13a)$$

subject to  $v_{\min} \leq v(\cdot) \leq v_{\max}$ ,

$$I_{\max}(s) := \sup_{v(\cdot) \in C([0, s])} I(v) \quad (13b)$$

subject to  $v_{\min} \leq v(\cdot) \leq v_{\max}$ ,

<sup>1</sup>Zonoids are defined as the range of an atom-free vector measure. These compact convex sets can be seen as the Hausdorff limit of a sequence of zonotopes (zonotopes are affine images of the unit cube); see e.g., [20]–[23].

and

$$I(v) := v(s) - \int_0^s f(\tau)v(\tau)d\tau, \quad f(\tau) := \langle \mathbf{c}, e^{(s-\tau)\mathbf{A}_{\text{con}}} \mathbf{b}_{\text{con}} \rangle. \quad (14)$$

In Sec. II-B, we semi-analytically determine  $I_{\min}(\cdot), I_{\max}(\cdot)$  from (13), and thereby  $u_{\min}(\cdot), u_{\max}(\cdot)$  from (12). In Sec. III, we derive parametric formula for the boundary  $\partial\mathcal{X}_t$  of the integrator reach set (10) with time-varying input range. They together complete **step 1**.

**Step 2** amounts to a simple computation: transform  $\mathcal{X}_t$  via a known linear map to obtain the desired  $\mathcal{Z}_t$ . This is justified because the map  $\mathbf{x} \mapsto \mathbf{z} = \mathbf{M}^{-1}\mathbf{x}$  is a homeomorphism, so the image of the boundary  $\partial\mathcal{X}_t$  is the boundary of the image  $\mathcal{Z}_t$ .

**Remark 1.** We note that the time-varying input range  $u_{\min}(\cdot), u_{\max}(\cdot)$  in (12) depends on both  $\mathbf{A}, \mathbf{b}$ . In particular, their dependence on  $\mathbf{b}$  occurs through the matrix  $\mathbf{M}$  in (2), which itself depends on  $\mathbf{b}$  via  $\mathbf{q}$ .

### B. Input Set in Brunovsky Coordinates

To determine the time-varying input range  $[u_{\min}(\cdot), u_{\max}(\cdot)]$ , we first express the function  $f$  in (14) as a *finite* sum involving the eigenvalues of the state matrix  $\mathbf{A}$ . This result is somewhat surprising since the  $f$  in (14) involves an *infinite* sum due to the matrix exponential.

**Lemma 1.** Suppose that the state matrix  $\mathbf{A} \in \mathbb{R}^{n \times n}$  has  $n$  distinct eigenvalues  $\lambda_1, \dots, \lambda_n \in \mathbb{C}$ . Then the function  $f$  in (14) can be expressed as

$$f(\tau) = - \sum_{i=1}^n \frac{\lambda_i^n}{\prod_{j \neq i} (\lambda_i - \lambda_j)} e^{\lambda_i(s-\tau)}, \quad 0 \leq \tau \leq s. \quad (15)$$

*Proof.* For convenience, let  $\theta := s - \tau$ . From (4), the vector  $e^{\theta\mathbf{A}_{\text{con}}} \mathbf{b}_{\text{con}}$  equals to the last column of the matrix exponential of  $\theta\mathbf{A}_{\text{con}}$ .

On the other hand,  $\mathbf{A}_{\text{con}}$  being a companion matrix, each consecutive row of  $e^{\theta\mathbf{A}_{\text{con}}}$  must be the derivative of its previous row w.r.t.  $\theta$ . Therefore, it suffices to determine the top right corner (i.e., first row and last column) entry of  $e^{\theta\mathbf{A}_{\text{con}}}$ , which we denote as  $g(\theta)$ .

We have

$$g(\theta) = (1 \quad 0 \quad 0 \quad \dots \quad 0) e^{\theta\mathbf{A}_{\text{con}}} \begin{pmatrix} 0 \\ 0 \\ \vdots \\ 0 \\ 1 \end{pmatrix} \\ = \sum_{r=0}^{\infty} (1 \quad 0 \quad 0 \quad \dots \quad 0) \frac{\theta^r \mathbf{A}_{\text{con}}^r}{r!} \begin{pmatrix} 0 \\ 0 \\ \vdots \\ 0 \\ 1 \end{pmatrix} \\ = \sum_{r=0}^{\infty} \frac{\theta^r}{r!} \sum_{i=1}^n \frac{\lambda_i^r}{p'(\lambda_i)}, \quad (16)$$

where the second line uses the Taylor series for matrix exponential,  $p'(\cdot)$  denotes the derivative of the characteristic polynomial  $p(\cdot)$  in (5), and the third line follows from a known result due to Dan Kalman [24, equation (9)] that gives a formula for the top right corner entry of the  $r$ th power of a companion matrix in terms of the eigenvalues. The latter result in turn comes from a connection between the powers of the companion matrix and the generalized Fibonacci sequences; see also [25], [26].

Exchanging the order of summation in (16), we get

$$g(\theta) = \sum_{i=1}^n \frac{1}{p'(\lambda_i)} \sum_{r=0}^{\infty} \frac{(\lambda_i \theta)^r}{r!} = \sum_{i=1}^n \frac{e^{\lambda_i \theta}}{p'(\lambda_i)}. \quad (17)$$

It follows that

$$e^{\theta \mathbf{A}_{\text{con}}} \mathbf{b}_{\text{con}} = \begin{pmatrix} g(\theta) \\ g^{(1)}(\theta) \\ \vdots \\ g^{(n-1)}(\theta) \end{pmatrix} \quad (18)$$

where the parenthetical superscript denotes the order of derivative w.r.t.  $\theta$ .

Combining (14), (17) and (18), we obtain

$$\begin{aligned} \langle \mathbf{c}, e^{\theta \mathbf{A}_{\text{con}}} \mathbf{b}_{\text{con}} \rangle &= \sum_{i=1}^n \frac{(c_0 + c_1 \lambda_i + \dots + c_{n-1} \lambda_i^{n-1}) e^{\lambda_i \theta}}{p'(\lambda_i)} \\ &= \sum_{i=1}^n \frac{(p(\lambda_i) - \lambda_i^n) e^{\lambda_i \theta}}{p'(\lambda_i)}. \end{aligned} \quad (19)$$

By definition,  $p(\lambda_i) = 0$ . Taking the logarithmic derivative of the characteristic polynomial  $p(\lambda) = \prod_{i=1}^n (\lambda - \lambda_i)$ , we have  $p'(\lambda_i) = \prod_{j=1, j \neq i}^n (\lambda_i - \lambda_j)$ . Substituting these back in (19), and recalling that  $\theta = s - \tau$ , the proof is complete. ■

**Example 1.** Let  $n = 2$  and  $\lambda_{1,2} = \rho e^{\pm \iota \phi}$ ,  $\iota := \sqrt{-1}$ , with  $\rho, \phi \neq 0$ . Then (15) gives

$$f(\tau) = -\frac{\rho}{\sin \phi} \sin(2\phi + (s - \tau)\rho \sin(2\phi)), \quad 0 \leq \tau \leq s.$$

**Example 2.** Let  $n = 3$  and  $\lambda_1 = 1$ ,  $\lambda_{2,3} = \pm \iota$ ,  $\iota := \sqrt{-1}$ . Then (15) gives

$$f(\tau) = -\frac{1}{2} (e^{s-\tau} + \cos(s - \tau) - \sin(s - \tau)), \quad 0 \leq \tau \leq s.$$

Theorem 1 presented next, shows that the zeros of the continuous function  $f$  become relevant for our purpose. For a fixed  $s \in (0, t]$ , the  $f$  in (15) may have multiple (Fig. 1), single or no<sup>2</sup> zeros in its domain  $[0, s]$ . At our level of generality, it is not possible to bound the number of such zeros in  $[0, s]$ , and we will numerically find the same.

Using Lemma 1, the following Theorem 1 quantifies how  $u_{\min}(s), u_{\max}(s)$ , and consequently the set  $\mathcal{Z}_t(\{\mathbf{z}_0\})$ , are determined by the integral of  $f$  over its zero sub-level and super-level sets.

**Theorem 1.** Suppose  $(\mathbf{A}, \mathbf{b})$  is a controllable pair and matrix  $\mathbf{A}$  has  $n$  distinct eigenvalues. For any  $0 \leq s \leq t$ ,

<sup>2</sup>as in Example 2, since  $e^\theta + \cos \theta - \sin \theta$  has no positive roots.

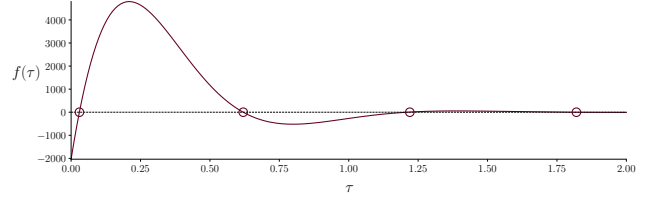


Fig. 1: The  $f(\tau)$  (solid line) in (15) for  $\mathbf{A} = \begin{bmatrix} 6 & 7 & 2 \\ -4 & -2 & 1 \\ -5 & 3 & 2 \end{bmatrix}$ , and its four zeros (circular markers) for  $\tau \in [0, 2]$ . Here  $\mathbf{A}$  has one real and two complex conjugate eigenvalues.

let  $\mathcal{L}_f^-$  (resp.  $\mathcal{L}_f^{++}$ ) denote the zero sublevel (resp. strict superlevel) set of  $f$  given by (15) over  $[0, s]$ , i.e.,

$$\mathcal{L}_f^- := \{\tau \in [0, s] \mid f(\tau) \leq 0\}, \quad (20a)$$

$$\mathcal{L}_f^{++} := \{\tau \in [0, s] \mid f(\tau) > 0\}. \quad (20b)$$

Then the  $I_{\min}(\cdot), I_{\max}(\cdot)$  in (12)-(13) can be computed as

$$I_{\min}(s) = v_{\min} - v_{\min} \int_{\tau \in \mathcal{L}_f^-} f(\tau) d\tau - v_{\max} \int_{\tau \in \mathcal{L}_f^{++}} f(\tau) d\tau, \quad (21a)$$

$$I_{\max}(s) = v_{\max} - v_{\max} \int_{\tau \in \mathcal{L}_f^-} f(\tau) d\tau - v_{\min} \int_{\tau \in \mathcal{L}_f^{++}} f(\tau) d\tau. \quad (21b)$$

Furthermore, the LTI reach set (11) with time-invariant input range  $[v_{\min}, v_{\max}]$  can be recovered from the integrator reach set (10) with time-varying input range  $[u_{\min}(s), u_{\max}(s)]$  given by (12), as

$$\mathcal{Z}_t(\{\mathbf{z}_0\}) = \mathbf{M}^{-1} \mathcal{X}_t(\{\mathbf{M} \mathbf{z}_0\}).$$

*Proof.* For a fixed finite  $s > 0$ , the function  $f(\tau)$  in (14) is continuous and bounded in  $\tau \in [0, s]$ . So  $v \mapsto I(v)$  is a continuous functional. Therefore, the infimum and supremum in (13) are achieved.

Because the functional  $I(v)$  in (14) is linear, we can determine the respective optimal values in terms of the disjoint union

$$[0, s] = \mathcal{L}_f^- \cup \mathcal{L}_f^{++}.$$

Using (13), (14) and Lemma 1, we arrive at (21).

The recovery of the LTI reach set (11) from the integrator reach set (10) follows from the input correspondence (7) and the subsequent discussion in Sec. II-A. ■

### III. PARAMETRIC BOUNDARY

Having determined the  $I_{\min}(\cdot), I_{\max}(\cdot)$  from (21), and therefore  $u_{\min}(\cdot), u_{\max}(\cdot)$  from (12), we now turn to deduce an explicit parameterization of the boundary  $\partial \mathcal{X}_t(\{\mathbf{x}_0\})$  for the integrator reach set  $\mathcal{X}_t(\{\mathbf{x}_0\})$  with input  $u \in [u_{\min}(s), u_{\max}(s)]$ ,  $0 \leq s \leq t$ .

In contrast to prior results in [9]–[11] where the input uncertainty were restricted to time-invariant sets, (12) requires us to consider a time-varying set  $[u_{\min}(s), u_{\max}(s)]$ . In this setting, Theorem 2 presented next, provides an explicit parameterization of  $\partial \mathcal{X}_t(\{\mathbf{x}_0\})$ , thus generalizing earlier developments in [9]–[11].

**Theorem 2.** Consider the integrator reach set (10) with time-varying range  $[u_{\min}(s), u_{\max}(s)]$ ,  $s \in [0, t]$ , given by (12) and (21). For  $k, \ell \in \mathbb{N}$ , let the indicator function  $\mathbf{1}_{k \leq \ell} := 1$  for  $k \leq \ell$ , and  $:= 0$  otherwise. Define a function  $\chi(t, \mathbf{x}_0) : \mathbb{R}_{>0} \times \mathbb{R}^n \mapsto \mathbb{R}^n$  component-wise:  $\chi^\ell := \sum_{k=1}^n \mathbf{1}_{k \leq \ell} \frac{t^{\ell-k}}{(\ell-k)!} \mathbf{x}_{\ell 0} \forall \ell \in \llbracket n \rrbracket$ , where  $\mathbf{x}_{\ell 0}$  denotes the  $\ell$ -th component of the initial state  $\mathbf{x}_0$ .

Let the parameter vector  $\boldsymbol{\sigma} = (\sigma_1, \sigma_2, \dots, \sigma_{n-1}) \in \mathcal{W}_t \subset \mathbb{R}^{n-1}$  where  $\mathcal{W}_t$  is the Weyl chamber:

$$\mathcal{W}_t := \{\boldsymbol{\sigma} \in \mathbb{R}^{n-1} \mid 0 \leq \sigma_1 \leq \sigma_2 \leq \dots \leq \sigma_{n-1} \leq t\}. \quad (22)$$

For  $0 \leq s \leq t$ , let

$$\mu(s) := (u_{\max}(s) - u_{\min}(s))/2, \quad (23a)$$

$$\nu(s) := (u_{\max}(s) + u_{\min}(s))/2, \quad (23b)$$

and

$$\boldsymbol{\xi}(s) := \begin{pmatrix} s^{n-1}/(n-1)! \\ s^{n-2}/(n-2)! \\ \vdots \\ s \\ 1 \end{pmatrix}. \quad (24)$$

Then,  $\mathbf{x}^{\text{bdy}} \in \partial \mathcal{X}_t(\{\mathbf{x}_0\})$  admits  $\boldsymbol{\sigma}$ -parameterization:

$$\begin{aligned} \mathbf{x}^{\text{bdy}}(\boldsymbol{\sigma}) &= \chi(t, \mathbf{x}_0) + \int_0^t \nu(s) \boldsymbol{\xi}(t-s) ds \pm \int_0^{\sigma_1} \mu(s) \boldsymbol{\xi}(t-s) ds \\ &\mp \int_{\sigma_1}^{\sigma_2} \mu(s) \boldsymbol{\xi}(t-s) ds \pm \dots \pm (-1)^n \int_{\sigma_{n-1}}^t \mu(s) \boldsymbol{\xi}(t-s) ds. \end{aligned} \quad (25)$$

*Proof.* Consider the support function  $h_{\mathcal{X}_t(\{\mathbf{x}_0\})}(\mathbf{y}) := \sup_{\mathbf{x} \in \mathcal{X}_t(\{\mathbf{x}_0\})} \langle \mathbf{y}, \mathbf{x} \rangle$  where  $\mathbf{y} \in \mathbb{S}^{n-1}$  (unit sphere in  $\mathbb{R}^n$ ). Generalizing our derivations in [11, Thm. 1], we find the support function of  $\mathcal{X}_t$  with time-varying input range  $[u_{\min}(s), u_{\max}(s)] \forall s \in [0, t]$ , as

$$\begin{aligned} h_{\mathcal{X}_t(\{\mathbf{x}_0\})}(\mathbf{y}) &= \left\langle \mathbf{y}, \chi(t, \mathbf{x}_0) + \int_0^t \nu(s) \boldsymbol{\xi}(t-s) ds \right\rangle \\ &+ \int_0^t \mu(s) |\langle \mathbf{y}, \boldsymbol{\xi}(t-s) \rangle| ds, \quad \mathbf{y} \in \mathbb{S}^{n-1}. \end{aligned} \quad (26)$$

Next, recall that the indicator function of any convex set is a convex function that is equal [27, Thm. 13.2] to the Legendre-Fenchel conjugate (denoted as  $h^*(\cdot)$ ) of its support function  $h(\cdot)$ . So, the boundary points  $\mathbf{x}^{\text{bdy}} \in \partial \mathcal{X}_t$  satisfy

$$\begin{aligned} h_{\mathcal{X}_t(\{\mathbf{x}_0\})}^*(\mathbf{x}^{\text{bdy}}) &= 0, \\ \Leftrightarrow \min_{\mathbf{y} \in \mathbb{S}^{n-1}} \left\{ \langle -\mathbf{x}^{\text{bdy}}, \mathbf{y} \rangle + h_{\mathcal{X}_t(\mathbf{x}_0)}(\mathbf{y}) \right\} &= 0. \end{aligned} \quad (27)$$

Using (26) and (24), we notice that the objective of the minimization problem in (27) contains an integral of the absolute value of the polynomial  $\langle \mathbf{y}, \boldsymbol{\xi}(\cdot) \rangle$ , which can have at most  $n-1$  roots, and therefore at most  $n-1$  sign changes occur within its domain  $[0, t]$ .

Let us denote the roots of this polynomial by  $\boldsymbol{\sigma} \in \mathcal{W}_t \subset \mathbb{R}^{n-1}$ . Then, this integral can be decomposed as a sum of  $n$  sub-integrals with alternate signs, whose upper and lower

limits are determined via  $\boldsymbol{\sigma}$  (see [11, eq. (62)] for details). As a result, the objective in (27) becomes linear in  $\mathbf{y}$ . Therefore, setting the coefficients of  $\mathbf{y}$  to zero, we obtain the parametric boundary (25).  $\blacksquare$

**Remark 2.** In the special case  $u_{\min}, u_{\max}$ , and thus  $\mu, \nu$  in (23) are constants, the parametric boundary formula (25) recovers [11, eq. (26)] via change of variable  $t-s \mapsto s$ .

The plus-minus appearing in the parameterization (25) has the following consequence.

**Corollary 3.** The integrator reach set (10) with time-varying range  $[u_{\min}(\cdot), u_{\max}(\cdot)]$  given by (12) and (21), has two bounding surfaces  $\partial \mathcal{X}_t^{\text{upper}}$  and  $\partial \mathcal{X}_t^{\text{lower}}$ , i.e.,

$$\partial \mathcal{X}_t(\{\mathbf{x}_0\}) := \partial \mathcal{X}_t^{\text{upper}}(\{\mathbf{x}_0\}) \cup \partial \mathcal{X}_t^{\text{lower}}(\{\mathbf{x}_0\}).$$

*Proof.* The bounding surfaces  $\partial \mathcal{X}_t^{\text{upper}}$  and  $\partial \mathcal{X}_t^{\text{lower}}$  correspond to two feasible choices of alternating signs in (25).

Specifically, if we consider the plus sign for the third summand in the right-hand side of (25), followed by alternating signs for the subsequent summands, we generate points on the upper boundary  $\partial \mathcal{X}_t^{\text{upper}}$ . Likewise, choosing the minus sign for the third summand in the right-hand side of (25), followed by alternating signs for the subsequent summands, generates points on the lower surface  $\partial \mathcal{X}_t^{\text{lower}}$ .  $\blacksquare$

**Remark 3.** From (25), the boundary  $\partial \mathcal{X}_t(\{\mathbf{x}_0\})$  only depends on the extremal curves  $u_{\min}(\cdot), u_{\max}(\cdot)$  of the time-varying input range.

**Remark 4.** Unlike the case of time invariant input range as in [10], [11], the integrator reach set  $\mathcal{X}_t$  with time-varying input range  $[u_{\min}(\cdot), u_{\max}(\cdot)]$ , though still a zonoid, is no longer semialgebraic in general. In fact, formula (25) shows that the zonoid  $\mathcal{X}_t$ , and therefore  $\mathcal{Z}_t$ , is semialgebraic iff  $u_{\min}(s), u_{\max}(s)$  are polynomials  $\forall 0 \leq s \leq t$ .

The following example illustrates how the above results can be brought together to compute the LTI reach set (11) via **step 1** and **step 2** mentioned in Sec. II-A.

**Example 3.** Consider the LTI reach set  $\mathcal{Z}_t$  in (11) at  $t=3$  with  $n=2$ ,  $\mathbf{z}_0 = \mathbf{0}_{2 \times 1}$ , for a system of the form (1):

$$\begin{pmatrix} \dot{z}_1 \\ \dot{z}_2 \end{pmatrix} = \underbrace{\begin{pmatrix} 0.1 & 0.2 \\ -0.3 & 0.1 \end{pmatrix}}_{\mathbf{A}} \begin{pmatrix} z_1 \\ z_2 \end{pmatrix} + \underbrace{\begin{pmatrix} 1 \\ 2 \end{pmatrix}}_{\mathbf{b}} v, \quad (28)$$

where the input ( $v(\cdot)$ ) trajectories are in  $\{v(\cdot) \in C([0, t]) \mid v(s) \in [-0.2, 0.2] \forall s \in [0, t]\}$ . So  $v_{\min} = -0.2, v_{\max} = 0.2$ .

To compute  $\mathcal{Z}_t$ , we follow **step 1** and **step 2** from Sec. II-A. Specifically, we have

$$\mathbf{M} = \begin{pmatrix} 20/11 & -10/11 \\ 5/11 & 3/11 \end{pmatrix}, \quad \mathbf{M}^{-1} = \begin{pmatrix} 3/10 & 1 \\ -1/2 & 2 \end{pmatrix}, \quad (29)$$

and (28) transforms to the controllable canonical form

$$\begin{pmatrix} \dot{x}_1 \\ \dot{x}_2 \end{pmatrix} = \underbrace{\begin{pmatrix} 0 & 1 \\ -0.07 & 0.20 \end{pmatrix}}_{\mathbf{A}_{\text{con}}} \begin{pmatrix} x_1 \\ x_2 \end{pmatrix} + \underbrace{\begin{pmatrix} 0 \\ 1 \end{pmatrix}}_{\mathbf{b}_{\text{con}}} v, \quad (30)$$

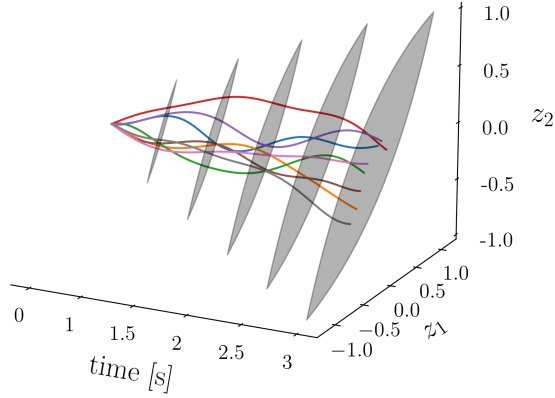


Fig. 2: The reach sets  $\mathcal{Z}_t(\{\mathbf{0}_{2 \times 1}\})$  at  $t = 1, 1.5, 2, 2.5, 3$  (grey filled) for **Example 3**. These sets were computed via the proposed two step method in Sec. II-A. The 8 sample state trajectories shown here correspond to 8 randomly sampled truncated Gaussian process input paths in  $\{v(\cdot) \in C([0, t]) \mid v(s) \in [-0.2, 0.2] \forall s \in [0, t]\}$ .

i.e.,  $\mathbf{c} := (0.07, -0.20)^\top$ . We find that  $\mathbf{A}$  has eigenvalues  $\lambda_{1,2} = \rho e^{\pm i\phi}$ ,  $\iota := \sqrt{-1}$ , with  $\rho = 0.2646$ ,  $\phi = 1.1832$ , and the  $f$  in (15) is as in **Example 1**.

With this  $f$ , we numerically compute  $I_{\min}(s), I_{\max}(s)$  from (21), and thereby the extremal trajectories  $u_{\min}(s), u_{\max}(s)$  from (12)  $\forall s \in [0, t = 3]$ . Using these  $u_{\min}(s), u_{\max}(s)$  and the initial condition  $\mathbf{x}_0 = \mathbf{M}\mathbf{z}_0 = \mathbf{0}_{2 \times 1}$ , we use (25) to explicitly compute  $\partial\mathcal{X}_t(\{\mathbf{0}_{2 \times 1}\})$ . We used trapezoidal approximations with step-size  $\Delta\tau = 0.01$  for evaluating the integrals in (21) and (25). This completes the **step 1**.

In **step 2**, we map  $\partial\mathcal{X}_t(\{\mathbf{0}_{2 \times 1}\})$  back to  $\partial\mathcal{Z}_t(\{\mathbf{0}_{2 \times 1}\})$  via the known linear map  $\mathbf{x}^{\text{bdy}} \mapsto \mathbf{M}^{-1}\mathbf{x}^{\text{bdy}} \in \partial\mathcal{Z}_t$ .

Fig. 2 plots the snapshots of  $\mathcal{Z}_t(\{\mathbf{0}_{2 \times 1}\})$  computed as above, at  $t = 1, 1.5, 2, 2.5$  and 3, together with 8 sample state trajectories of (28) with the same zero initial state. These sample state trajectories correspond to 8 randomly sampled truncated Gaussian process input paths in  $\{v(\cdot) \in C([0, t]) \mid v(s) \in [-0.2, 0.2] \forall s \in [0, t]\}$ .

#### IV. VOLUME

Building on **step 1** and **step 2** from Sec. II-A, we now show that the same ideas also help computing the volume of the LTI reach set, i.e.,  $\text{vol}_n(\mathcal{Z}_t(\{\mathbf{z}_0\}))$ .

As discussed in earlier works [9], [11, Sec. VI], having a computational handle on volume is helpful in providing ground truth to quantify the conservatism of numerical algorithms which over-approximate the reach set via simpler geometric shapes such as variants of ellipsoids [28]–[32] or variants of zonotopes [4], [33]–[38].

We start by noticing that each  $\boldsymbol{\sigma} \in \mathcal{W}_t$  assigns a pair of points  $(\mathbf{x}^{\text{upper}}, \mathbf{x}^{\text{lower}})$  on  $\partial\mathcal{X}_t$ , one on each bounding hypersurfaces mentioned in Corollary 3, i.e.,  $\mathbf{x}^{\text{upper}}(\boldsymbol{\sigma}) \in \partial\mathcal{X}^{\text{upper}}(\boldsymbol{\sigma})$  and  $\mathbf{x}^{\text{lower}}(\boldsymbol{\sigma}) \in \partial\mathcal{X}^{\text{lower}}(\boldsymbol{\sigma})$ .

Since  $\mathcal{X}_t$  is convex, each  $\mathbf{x} \in \mathcal{X}_t$  can be written as a convex combination of two points in  $\mathcal{X}_t$ . In the following, we show a stronger result: any point in  $\mathcal{X}_t$  can be written as a convex combination of a pair  $(\mathbf{x}^{\text{upper}}, \mathbf{x}^{\text{lower}})$  evaluated at the same parameter  $\boldsymbol{\sigma} \in \mathcal{W}_t$ . This result will find use in volume computation (Thm. 5).

**Theorem 4.** For any  $\mathbf{x} \in \mathcal{X}_t$ , there exists  $(\boldsymbol{\sigma}, \lambda) \in \mathcal{W}_t \times [0, 1]$  such that

$$\mathbf{x} = \boldsymbol{\pi}(\boldsymbol{\sigma}, \lambda) := \lambda \mathbf{x}^{\text{upper}}(\boldsymbol{\sigma}) + (1 - \lambda) \mathbf{x}^{\text{lower}}(\boldsymbol{\sigma}), \quad (31)$$

i.e., the parametric map  $\boldsymbol{\pi} : \mathcal{W}_t \times [0, 1] \rightarrow \mathcal{X}_t$  is surjective.

*Proof.* Let us denote the summation of the first two constant terms in the right-hand-side of (25) as  $\boldsymbol{\eta}_t$ . W.l.o.g., we prove our claim in a translated coordinate system with origin at  $\boldsymbol{\eta}_t$ .

Notice that the bounding hypersurfaces in (25) have an antipodal property, i.e., for any fixed  $\boldsymbol{\sigma} \in \mathcal{W}_t$ , the line segment  $\ell(\boldsymbol{\sigma}) := \lambda \mathbf{x}^{\text{upper}}(\boldsymbol{\sigma}) + (1 - \lambda) \mathbf{x}^{\text{lower}}(\boldsymbol{\sigma})$  generated by varying  $\lambda \in [0, 1]$ , will pass through the origin. Since  $\mathcal{X}_t$  is convex and compact, for any  $\tilde{\mathbf{x}} \in \mathcal{X}_t$ , the line through  $\tilde{\mathbf{x}}$  and the origin crosses the boundary at the antipodal points  $\tilde{\mathbf{x}}^{\text{upper}} = \mathbf{x}^{\text{upper}}(\boldsymbol{\sigma})$  and  $\tilde{\mathbf{x}}^{\text{lower}} = \mathbf{x}^{\text{lower}}(\boldsymbol{\sigma})$  for some  $\boldsymbol{\sigma} \in \mathcal{W}_t$ . Therefore,  $\tilde{\mathbf{x}} \in \ell(\boldsymbol{\sigma})$ . It follows that  $\boldsymbol{\pi}$  is surjective. ■

**Remark 5.** We clarify here that (25) gives a parameterization of  $\partial\mathcal{X}_t$ , while (31) gives a parameterization of  $\mathcal{X}_t$ .

**Theorem 5.** The  $n$  dimensional Lebesgue volume of the LTI reach set (11) at time  $t$ , is

$$\text{vol}_n(\mathcal{Z}_t(\{\mathbf{z}_0\})) = \frac{1}{|\det(\mathbf{M})|} \int_0^1 \int_{\mathcal{W}_t} |\det(\mathbf{D}\boldsymbol{\pi})| d\boldsymbol{\sigma} d\lambda \quad (32)$$

where the nonsingular  $\mathbf{M} \in \mathbb{R}^{n \times n}$  is given by (2),  $\mathbf{D}\boldsymbol{\pi}$  denotes the Jacobian of  $\boldsymbol{\pi}$  in (31), and  $\boldsymbol{\sigma} \in \mathcal{W}_t$  as in (22). In particular,

$$|\det(\mathbf{D}\boldsymbol{\pi})| = \mu(\sigma_1)\mu(\sigma_2)\dots\mu(\sigma_{n-1})(4\lambda - 2)^{n-1} \left| \det \begin{pmatrix} \frac{(t - \sigma_1)^{n-1}}{(n-1)!} & \dots & \frac{(t - \sigma_{n-1})^{n-1}}{(n-1)!} & \zeta_1(\boldsymbol{\sigma}) \\ \vdots & \vdots & \vdots & \vdots \\ (t - \sigma_1) & \dots & (t - \sigma_{n-1}) & \zeta_{n-1}(\boldsymbol{\sigma}) \\ 1 & \dots & 1 & \zeta_n(\boldsymbol{\sigma}) \end{pmatrix} \right|, \quad (33)$$

where  $\zeta(\boldsymbol{\sigma}) := \mathbf{x}^{\text{upper}}(\boldsymbol{\sigma}) - \mathbf{x}^{\text{lower}}(\boldsymbol{\sigma})$ .

*Proof.* Since  $\mathcal{Z}_t(\{\mathbf{z}_0\}) = \mathbf{M}^{-1}\mathcal{X}_t(\{\mathbf{M}\mathbf{z}_0\})$ , and  $\text{vol}_n$  is translation invariant, we have

$$\text{vol}_n(\mathcal{Z}_t(\{\mathbf{z}_0\})) = \frac{1}{|\det(\mathbf{M})|} \text{vol}_n(\mathcal{X}_t(\{\mathbf{0}\})). \quad (34)$$

So it suffices to compute  $\text{vol}_n(\mathcal{X}_t(\{\mathbf{0}\}))$ .

Using the parameterization (31), we get

$$d \text{vol}_n \mathcal{X}_t(\mathcal{X}_t(\{\mathbf{0}\})) = |\det(\mathbf{D}\boldsymbol{\pi})| d\sigma_1 \dots d\sigma_{n-1} d\lambda. \quad (35)$$

From (31), the map  $\boldsymbol{\pi}$  is  $C^1(\mathcal{W}_t \times [0, 1])$ . By Sard's theorem [39, Ch. 2], the set of critical values (image of the set of critical points in  $\mathcal{W}_t \times [0, 1]$  where  $\det(\mathbf{D}\boldsymbol{\pi}) = 0$ ) has  $n$  dimensional Lebesgue measure zero. Therefore, (34)–(35) yield (32).

Using (25) and Corollary 3, direct computation gives

$$|\det(\mathbf{D}\boldsymbol{\pi})| = \left| \det \begin{pmatrix} \frac{\partial \boldsymbol{\pi}(\boldsymbol{\sigma}, \lambda)}{\partial \boldsymbol{\sigma}} & \frac{\partial \boldsymbol{\pi}(\boldsymbol{\sigma}, \lambda)}{\partial \lambda} \end{pmatrix} \right| = (33).$$

This completes the proof. ■

**Example 4.** Consider the reach set  $\mathcal{Z}_t(\{\mathbf{0}_{2 \times 1}\})$  for (28) at  $t = 3$  as in Example 3. We have

$$\zeta_1 = 2 \left( \int_0^{\sigma_1} (t - \tau) d\tau - \int_{\sigma_1}^t (t - \tau) d\tau \right) = t^2 - 2(t - \sigma_1)^2,$$

$$\zeta_2 = 2 \left( \int_0^{\sigma_1} d\tau - \int_{\sigma_1}^t d\tau \right) = 4\sigma_1 - 2t.$$

Thus (33) becomes

$$\begin{aligned} |\det(D\pi)| &= \mu(\sigma_1) |4\lambda - 2| \left| \det \begin{pmatrix} t - \sigma_1 & t^2 - 2(t - \sigma_1)^2 \\ 1 & 4\sigma_1 - 2t \end{pmatrix} \right| \\ &= \mu(\sigma_1) |4\lambda - 2| |-\sigma_1^2 - (t - \sigma_1)^2|. \end{aligned} \quad (36)$$

Using (29) and (36), formula (32) then yields

$$\begin{aligned} \text{vol}_2(\mathcal{Z}_3) &= \frac{11}{10} \int_0^1 \int_{\sigma_1}^3 \mu(\sigma_1) |4\lambda - 2| (\sigma_1^2 + (3 - \sigma_1)^2) d\sigma_1 d\lambda \\ &\approx 0.3043, \end{aligned}$$

using the same  $\mu(\cdot)$  as in Example 3, and the trapezoidal method with step-size  $\Delta\tau = 0.01$  to estimate the integral.

## V. CONCLUDING REMARKS

This work demonstrates that the boundary and volume of a controllable single input LTI reach set with *time-invariant* input range can be computed from the boundary and volume of an integrator reach set with a *time-varying* input range induced by the LTI system. Extending this line of ideas for multi-input LTI systems will comprise our future work.

## REFERENCES

- [1] T. Pecsvaradi and K. S. Narendra, "Reachable sets for linear dynamical systems," *Information and control*, vol. 19, no. 4, pp. 319–344, 1971.
- [2] H. Witsenhausen, "A remark on reachable sets of linear systems," *IEEE Transactions on Automatic Control*, vol. 17, no. 4, pp. 547–547, 1972.
- [3] P. Varaiya, "Reach set computation using optimal control," in *Verification of Digital and Hybrid Systems*. Springer, 2000, pp. 323–331.
- [4] A. Girard, "Reachability of uncertain linear systems using zonotopes," in *International Workshop on Hybrid Systems: Computation and Control*. Springer, 2005, pp. 291–305.
- [5] A. Girard, C. Le Guernic, and O. Maler, "Efficient computation of reachable sets of linear time-invariant systems with inputs," in *Hybrid Systems: Computation and Control: 9th International Workshop, HSCC 2006, Santa Barbara, CA, USA, March 29-31, 2006. Proceedings 9*. Springer, 2006, pp. 257–271.
- [6] A. A. Kurzhanskiy and P. Varaiya, "Ellipsoidal techniques for reachability analysis of discrete-time linear systems," *IEEE Transactions on Automatic Control*, vol. 52, no. 1, pp. 26–38, 2007.
- [7] S. Kaynama and M. Oishi, "Schur-based decomposition for reachability analysis of linear time-invariant systems," in *Proceedings of the 48th IEEE Conference on Decision and Control (CDC) held jointly with 2009 28th Chinese Control Conference*. IEEE, 2009, pp. 69–74.
- [8] M. Althoff, G. Frehse, and A. Girard, "Set propagation techniques for reachability analysis," *Annual Review of Control, Robotics, and Autonomous Systems*, vol. 4, pp. 369–395, 2021.
- [9] S. Haddad and A. Halder, "The convex geometry of integrator reach sets," in *2020 American Control Conference (ACC)*. IEEE, 2020, pp. 4466–4471.
- [10] S. Haddad and A. Halder, "Boundary and taxonomy of integrator reach sets," in *2022 American Control Conference (ACC)*. IEEE, 2022, pp. 4133–4138.
- [11] S. Haddad and A. Halder, "The curious case of integrator reach sets, part i: Basic theory," *IEEE Transactions on Automatic Control*, 2023.
- [12] S. Haddad and A. Halder, "Certifying the intersection of reach sets of integrator agents with set-valued input uncertainties," *IEEE Control Systems Letters*, vol. 6, pp. 2852–2857, 2022.
- [13] P. Antsaklis and A. Michel, *A Linear Systems Primer*. Massachusetts: Birkhauser, 2007.
- [14] R. A. Horn and C. R. Johnson, *Matrix analysis*. Cambridge university press, 2012.
- [15] A. Liapounoff, "Sur les fonctions-vecteurs completement additives," *Izvestiya Rossiiskoi Akademii Nauk. Seriya Matematicheskaya*, vol. 4, no. 6, pp. 465–478, 1940.
- [16] P. R. Halmos, "The range of a vector measure," *Bulletin of the American Mathematical Society*, vol. 54, no. 4, pp. 416–421, 1948.
- [17] Z. Artstein, "Yet another proof of the Lyapunov convexity theorem," *Proceedings of the American Mathematical Society*, vol. 108, no. 1, pp. 89–91, 1990.
- [18] I. Ekeland, P. Marcellini, A. Marino, M. Tosques, C. Olech, G. Pini-giani, T. Rockafeller, M. Valadier, and C. Olech, "The Lyapunov theorem: its extensions and applications," in *Methods of Nonconvex Analysis: Lectures given at the 1st Session of the Centro Internazionale Matematico Estivo (CIME) held at Varenna, Italy, June 15–23, 1989*. Springer, 1990, pp. 84–103.
- [19] J. Yong and X. Y. Zhou, *Stochastic controls: Hamiltonian systems and HJB equations*. Springer Science & Business Media, 1999, vol. 43.
- [20] E. D. Bolker, "A class of convex bodies," *Transactions of the American Mathematical Society*, vol. 145, pp. 323–345, 1969.
- [21] R. Schneider and W. Weil, "Zonoids and related topics," *Convexity and its Applications*, pp. 296–317, 1983.
- [22] P. Goodey and W. Wolfgang, "Zonoids and generalisations," in *Handbook of convex geometry*. Elsevier, 1993, pp. 1297–1326.
- [23] J. Bourgain, J. Lindenstrauss, and V. Milman, "Approximation of zonoids by zonotopes," *Acta Mathematica*, vol. 162, no. 1, pp. 73–141, 1989.
- [24] D. Kalman, "Generalized Fibonacci numbers by matrix methods," *Fibonacci Quart*, vol. 20, no. 1, pp. 73–76, 1982.
- [25] W. Y. Chen and J. D. Louck, "The combinatorial power of the companion matrix," *Linear Algebra and its Applications*, vol. 232, pp. 261–278, 1996.
- [26] R. B. Taher and M. Rachidi, "On the matrix powers and exponential by the  $r$ -generalized Fibonacci sequences methods: the companion matrix case," *Linear Algebra and Its Applications*, vol. 370, pp. 341–353, 2003.
- [27] R. T. Rockafellar, *Convex analysis*. Princeton university press, 1997, vol. 11.
- [28] A. Kurzhanski and I. Vályi, *Ellipsoidal calculus for estimation and control*. Springer, 1997.
- [29] C. Durieu, E. Walter, and B. Polyak, "Multi-input multi-output ellipsoidal state bounding," *Journal of optimization theory and applications*, vol. 111, pp. 273–303, 2001.
- [30] A. Halder, "On the parameterized computation of minimum volume outer ellipsoid of Minkowski sum of ellipsoids," in *2018 IEEE Conference on Decision and Control (CDC)*. IEEE, 2018, pp. 4040–4045.
- [31] A. Halder, "Smallest ellipsoid containing  $p$ -sum of ellipsoids with application to reachability analysis," *IEEE Transactions on Automatic Control*, vol. 66, no. 6, pp. 2512–2525, 2020.
- [32] S. Haddad and A. Halder, "Anytime ellipsoidal over-approximation of forward reach sets of uncertain linear systems," in *Proceedings of the Workshop on Computation-Aware Algorithmic Design for Cyber-Physical Systems*, 2021, pp. 20–25.
- [33] M. Althoff and B. H. Krogh, "Zonotope bundles for the efficient computation of reachable sets," in *2011 50th IEEE conference on decision and control and European control conference*. IEEE, 2011, pp. 6814–6821.
- [34] M. Althoff, "An introduction to CORA 2015," *ARCH@ CPSWeek*, vol. 34, pp. 120–151, 2015.
- [35] J. K. Scott, D. M. Raimondo, G. R. Marseglia, and R. D. Braatz, "Constrained zonotopes: A new tool for set-based estimation and fault detection," *Automatica*, vol. 69, pp. 126–136, 2016.
- [36] N. Kochdumper and M. Althoff, "Sparse polynomial zonotopes: A novel set representation for reachability analysis," *IEEE Transactions on Automatic Control*, vol. 66, no. 9, pp. 4043–4058, 2020.
- [37] S. Kousik, A. Dai, and G. X. Gao, "Ellipsotopes: Uniting ellipsoids and zonotopes for reachability analysis and fault detection," *IEEE Transactions on Automatic Control*, 2022.
- [38] N. Kochdumper, C. Schilling, M. Althoff, and S. Bak, "Open-and closed-loop neural network verification using polynomial zonotopes," in *NASA Formal Methods Symposium*. Springer, 2023, pp. 16–36.
- [39] J. Milnor and D. W. Weaver, *Topology from the differentiable viewpoint*. Princeton university press, 1997, vol. 21.